# Liquid chromatography/tandem mass spectrometric characterization of Rhodotorula mucilaginosa GMM natural pigment and its synergistic antitumor effect with $\gamma$ -radiation: in-vitro and in-vivo study

Ghada S. Ibrahim<sup>a</sup>, Amal I. Hassan<sup>b</sup>, Manal G. Mahmoud<sup>a</sup>, Mohsen M.S. Askera, Mohamed Marzoukc

<sup>a</sup>Department of Microbial Biotechnology, Biotechnology Research Institute, National Research Centre, Dokki, Cairo, Egypt, bDepartment of Radioisotopes, Nuclear Research Centre, Egyptian Atomic Energy Authority, Cairo, Egypt, <sup>c</sup>Department of Chemistry of Tanning Materials and Leather Technology, Chemical Industries Research Institute, National Research Centre, Dokki, Cairo, Egypt

Correspondence to Mohsen M.S. Asker, PhD, Department of Microbial Biotechnology, Biotechnology Research Institute, National Research Centre, 33 Bohouth Street, Dokki, Giza 12622, Egypt. Tel: 00201229552825; fax: 0233371615;

e-mail: mohsenmsa@yahoo.com

Received: 16 April 2024 Revised: 30 May 2024 Accepted: 2 June 2024 Published: 24 December 2024

Journal of The Arab Society for Medical

Research 2024, 19:167-185

### Background/aim

Recently, there has been a marked increase in interest toward using microbial resources, especially yeast, to synthesize carotenoids. Ovarian cancer is a major health problem worldwide, as it is the most frequently diagnosed form of cancer in women and contributes significantly to cancer-related deaths. Yeast carotenoids are currently under evaluation for cost-effective and nonhazardous drugs derived from natural products. The principal objective of this study is to evaluate the natural pigment produced from Rhodotorula and characterize it by liquid chromatographymass spectrometric and to evaluate the ability of its synergistic antitumor effect with  $\gamma$ -radiation.

#### Materials and methods

A new pigmented yeast was isolated from yogurt and identified. The pigment was characterized and studies of its biological activities were conducted. The isolate was defined as Rhodotorula mucilaginosa GMM with accession number OQ120277 by 18 S rDNA, and the pigment was characterized by liquid chromatography-mass spectrometric. Combining γ-radiation with a carotenoid pigment was also tested for its synergistic anticancer properties in CAOV-3 and HEK-293 cell lines and in experimental mice bearing solid tumors. BAX, BCL2, P53, MMP2, MMP9, caspase-3, and caspase-9 were measured using ELISA techniques.

### Results

The maximum production of total carotenoids was 2.99 g/l. Pigment extract constituents exhibited 12 major compounds during its identification. Their structures can be sorted as 8 tetra, and 3 triterpenoidal carotenes (astaxanthin, 4,4'-E-diapophytoene, torularhodin, 1,2,1',2'-tetrahyroxylycopene, E-β-apo-8'-10'-apo-E-β-caroten-10'-ol, β-carotene, torulene, echinenone, 1,2,1',2'-tetrahyroxy dihydrolycopene, and α-canthaxanthin). The pigment exhibited DPPH scavenging activity, and the combination of natural pigment and radiation therapy showed a significant reduction (P < 0.05) in the levels of matrix metalloproteinases (MMP2, MMP9), and significant increases (P<0.05) in the levels of tumor protein p53, Bax and caspases-3 and caspases-9 in CAOV-3 cell lines and mice bearing solid tumors.

#### Conclusion

The natural pigment produced by yeast fermentation in this study exhibited a potential antitumor efficacy when combined with radiation in cell lines and against Ehrlich solid tumors.

#### **Keywords:**

antiproliferative, apoptosis, carotenoids, liquid chromatography-mass spectrometric, ovarian cancer, Rhodotorula mucilaginosa, γ-radiation

J Arab Soc Med Res 19:167-185 © 2024 Journal of The Arab Society for Medical Research 1687-4293

#### Introduction

Cancer is the leading cause of death and a major public health issue in most regions of the world, claiming more than six million lives each year [1]. Cancer incidence is expected to rise to 22.2 million cases by 2030. The most lethal stage of the cancer procedure, metastasis, seems to rely on macrophages, the robust immune system cells that normally fight illness energetically. If these unique macrophages are eliminated, metastatic tumor development will be slowed. Furthermore, metastatic cancer is the

This is an open access journal, and articles are distributed under the terms of the Creative Commons Attribution-NonCommercial-ShareAlike 4.0 License, which allows others to remix, tweak, and build upon the work non-commercially, as long as appropriate credit is given and the new creations are licensed under the identical terms.

leading cause of cancer death [2]. Cancer requires a unique treatment plan that may involve one or more of the following methods such as surgery, radiation, chemotherapy, hormone therapy, immunotherapy, and targeted therapy, with targeted therapy referring to drugs that precisely interfere with cancer cells in the patient [3]. Further research was required to find novel treatment chemicals that were more effective, safe, and selective to win the war against this devastating illness. As a result, new kinds of cancer medications are required.

Nowadays, pigments are used in many areas, such as medicine, food, ink, paper, textiles, aquaculture, and animal feed [4]. Since the discovery of the harmful health consequences of synthetic colorants, which have been used in food for a long time, scientists and consumers have favored natural colorants. The antibacterial, antioxidant, and anticancer properties of natural colorants are attracting more and more attention daily. Carotenoids' antioxidants can change bio middles, strengthen the lipid bilayer, and reduce its fluidity, all blocking carcinogenesis from starting [5]. By removing reactive oxygen species (ROS) from the human body, natural carotenoids like β-carotene aid in defensive mechanisms. Moreover, carotenoids suppress cell proliferation, stimulate detoxifying enzymes, and upregulate gap junction communication [6]. The significant financial outlay is the primary deterrent to the widespread use of natural colorants in food and as anticancer pigment agents. The comparative ease with which microbes and lower plants grow makes biotechnology methods for producing carotenoids preferable to synthetic ones [7].bioprocesses Therefore, producing using microorganisms with a reasonably high growth speed is preferable, as this can guarantee process productivity. Pigment-producing microorganisms common in nature and rich in color. Their different chemical compositions and the presence of specific chromophores are the reasons for the diversity of pigments Streptomyces chrestomyceticus, [8-10].Blakeslea trispora, **Phycomyces** blakesleeanus, Flavobacterium sp., Phaffia sp., and Rhodotorula sp. are defined as carotenoid-producing microorganisms [11-13]. Pigmented basidiomycetous yeasts of the genus Rhodotorula are easily identifiable by their distinctive colonies that are yellow, orange, or/and red [11].

Isolation of natural products in pure form from their natural sources, that is, plant, animal, or microbial cultural sources, is necessary using one highperformance separation chromatographic technique (e.g. HPTLC, CE, or HPLC) and one and/or more of the different spectrometric tools [14,15]. The liquid chromatography-mass spectrometric (LC-MS) technique is a fast analytical characterization tool for their complex microbial pigments [16,17].

Gamma irradiation is thought to be a form of physical stress on living organisms or cells. Radiation therapy can be a much quicker technique to boost the quantitative production of antioxidant molecules that may play a role in safeguarding irradiated tissue [18]. Oxidative stress species (ROS) can alter several metabolic processes, particularly those connected to oxidative stress [19]. It is well known that carotenoids have several uses, including fighting cancer, boosting the immune system, coloring sausage, soda, and baked products, and adding them to cosmetics. The discovery of the harmful health effects of synthetic colorants, which have been used in food for a long time, prompted scientists and consumers to focus on natural colorants. In both clinical trials and preclinical research, some natural compounds have been shown to lessen the side effects of chemotherapy and radiotherapy on the mouth, the digestive system, the liver, the kidneys, the heart, and the nerves.

Therefore, this study is designed to evaluate the capacities of the naturally produced pigment by isolating the Rhodotorula mucilaginous from yogurt and optimizing the UPLC-HRESI-qTOF-MS/MS main system as a tool for its chemical characterization and evaluation of the ability of γ-radiation and extracted pigment in facing cancer cells and inhibiting cell growth in the CAOV-3 cell line in vitro and solid tumors in mice.

# Materials and methods Materials

Sigma-Aldrich provided the 2,2-diphenyl-1picrylhydrazyl (DPPH), fluorescein, 6-hydroxy-2,5,7,8-tetramethylchroman-2-carboxylic acid (Trolox), and 2,2'-azobis(2-amidinopropane) dihydrochloride (AAPH) (St. Louis, Missouri, USA). All of the chemicals and solvents used are of the analytical grade. Whole-body γ-irradiation of mice and the human ovarian cancer cell line CAOV-3 (ATCC HTB-75) were performed with a Canadian gamma cell 40 (137Cs) at the National Center for Radiation Research and Technology, Cairo, Egypt.

#### **Experimental animals**

Female Swiss adult albino mice weighing 22–25 g were obtained from the National Centre for Radiation

Research and Technology Animal Facility in Cairo, Egypt. The animals were fed a regular pellet diet, and water was given ad libitum, and kept under a 12-12 dark-light cycle under normal pressure temperature conditions.

# Ethical approved

All the experiments were done in compliance with the Public Health Guide for the Care and Use of Laboratory Animals and were performed in line with the guidelines of ethical conditions approved by the Research Ethics Committee of the National Center for Radiation Research and Technology in Egypt under reference number 37 A/23.

#### Methods

# Isolation of pigmented yeast

The pigment-producing strain of our study was isolated from yogurt bought from the local market in Egypt and left in the refrigerator for 30 days. Isolation was carried out on a 5% glycerol nutrient agar medium and incubated at 25°C for at least 1 day. Colonies of distinct colors on agar plates identified the pigment-producing isolate. The pure pigmented isolate was picked and stored in a 5% glycerol nutrient agar. The isolate was identified using the 18 s rRNA gene.

# Molecular characterization of the isolate pigment

The yeast strain responsible for producing the orange pigment is isolated from the surface of old, cold yogurt using the plating process, and the morphological characteristics of the isolated yeast allowed for its identification [20]. The yeast biomass was collected from 1 ml of grown NA+glycerol 5% cultures by centrifugation at 10 000 rpm for 10 min. The DNA extraction was performed using a DNA extraction kit, and the quality was assessed using a 1.2% agarose gel. A single band of high molecular weight DNA was found. The DNA that was obtained was utilized as a template for PCR. The 18 S rDNA gene was PCR amplified using the following primers, namely ITS1 (5'-TCCG TAGGTGAACCTGCGG-3') and ITS4 (5'-TCCT CCGCTTATTGATATGC-3') [21]. After that, partial sequencing was performed at the Macrogen Company, Korea. Taxonomic identification of producing strains will be served with phylogenic analysis. Nucleotide sequences were compared with GenBank databases using the BLASTN program available on the NCBI, followed by sequence alignment. A phylogenetic tree was constructed using the neighbor-joining algorithm and 1000 resamplings in the Molecular Evolutionary Genetic Analysis, version 5.2 software.

### **Bioproduction of pigment**

The yeast-rich pigment was synthesized using nutrient broth (NB) with a 5% glycerol concentration. The generation of cellular biomass was carried out in two consecutive stages. Initially, a volume of 600 ml of NB medium was contaminated with 10 ml of isolated colored yeast and subjected to incubation for 48 h at a temperature of 25°C and a speed of 100 rpm. After the incubation period, the entire 10 ml of the infected medium was combined with 600 ml of sterile NB containing 5% glycerol in a bioreactor with a total volume of 2 L. The culture was cultivated at 25°C and a pH of 5.5 for 3 days. Aeration was provided at a rate of 0.5 vvm, and the agitation speed was set at 360 rpm. The cell pellets were reconstituted with distilled water and then centrifuged at 4000 rpm for 10 min to separate the cells from the supernatant. Yeast cells were harvested to determine the concentration of pigments.

#### Extraction and characterization of the biopigment

A 1 ml culture was diluted to 10 ml using 25% NaCl to cell growth  $\mathrm{OD}_{660\mathrm{nm}}$ spectrophotometer [22]. Yeast cells were harvested by centrifugation at 4000 rpm for 15 min, and then abrasion with glass pearls was the adapted method [23]. Cells (0.5 g) were mixed with 6 ml acetone, frozen for 48 h after glass pearls were added and crashed in a mortar, and then agitated vigorously for 5 min; this process was repeated thrice. After cell disruption, the supernatant was separated by centrifugation (4000 rpm for 15 min) for subsequent carotenoid extraction. Methanol was added to the disrupted cells and agitated vigorously for 5 min by a vortex agitator. This process was repeated three times to complete the extraction of the pigment (GMMP). The GMMP was scanned at 200-800 nm using the Shimadzu UV-2401PC spectrophotometer. The solvent was evaporated entirely at 37°C, and the -20°C [24]. pigment was stored at pigmentation degree was determined by calculating the ratio of carotenoid  $OD_{\lambda max}$  to growth  $OD_{660nm}$ .

# Cells dry weight determination

A yeast culture of 50 ml was subjected to centrifugation for 20 min at 4000 rpm. The resulting pellet was washed two times with distilled water and dried at 80°C until constant weight [24].

# Liquid chromatography-mass spectrometric

An exhaustive metabolomics investigation nontargeting small molecules was conducted on the pigment sample extract, prepared as below, for LC/MS Proteomics measurements and Metabolomics

#### In-vitro study

# Assessment of the antioxidant capacity of the extracted pigment

DPPH radical scavenging activity: the radical scavenging activity of the methanol GMMP was assessed using the DPPH assay to determine its antioxidant potential. The extract's antioxidant potential was confirmed by its ability to donate hydrogen or scavenge radicals [26]. Pigment at different concentrations (2.0, 4.0, 6.0, 8.0, and 10 mg/ml) and ascorbic acid at 20–100 µg/ml were prepared in methanol. The inhibition percentage was calculated using the following formula:

Scavenging activity(%) =  $Ac - As/Ac \times 100$  where Ac is the absorbance of the control and As is the absorbance of the sample.

# Oxygen radical scavenging capacity

The procedure followed the methodology described in Liang *et al.* [27]. A measure of 10 ml of GMMP was mixed with 30 ml of fluoresceine (100 nM) and left to sit for 10 min at 37°C. Results of the samples are presented as  $\mu$ M TE/mg sample using the linear

regression equation extracted from the following calibration curve (linear dose-inhibition curve of Trolox). Moreover, for the background measurement, three cycles of fluorescence measurement (485 EX, 520 EM, and nm) were performed with a cycle time of 90 s each. After that,  $70\,\mu l$  of  $300\,mM$  2,2'-Azobis(2-amidinopropane) dihydrochloride (AAPH) was added to the MSTh well right away. After 60 min of 40 cycles of 90 s of MSTh, the fluorescence measurement stayed at 485 EX and 520 EM nm. We presented the data as the mean of three samples.

# Cell culture protocols

The human ovarian cancer cell line CAOV-3 (ATCC HTB-75) and the normal human embryonic kidney cell line HEK-293 were obtained from the Department of Microbiology (Viruses), Faculty of Medicine, Al-Azhar University, Cairo, Egypt. The cells were cultured in RPMI medium supplemented with 100 mg/ml streptomycin, 100 U/ml penicillin, and 10% heat-inactivated fetal bovine serum at 37°C in a humidified, 5% (v/v) CO<sub>2</sub> environment. Only sterile equipment contacted the cells directly during cell testing in a laminar flow. The culture was restarted once the cells had reached 80-90% confluence after 2 days. The media was removed by aspiration, and the cells were rinsed three times with phosphate-buffered saline before being divided (pH 7.4). PBS was withdrawn from the flasks and replaced with 0.025% trypsin EDTA. The flasks were incubated in the incubator for 3-5 min before the cells were released. The cells were then diluted to the required concentration before being grown in new flasks.

# Cell count

Trypan blue was a dye used to determine viable versus nonviable cells. The nonviable cells stained dark blue by taking up the dye [28]. The cell suspension was diluted 1:1 and pipetted several times in trypan blue to ensure homogeneous suspensions. The suspension was loaded the two counting chambers hemocytometer. The cells were distributed in 96well plates with a density of 5000 cells per well. The experiment involved exposing CAOV-3 cancer cell lines to various concentrations of the GMMP (0, 5, 10, 20, and 50  $\mu$ g/ml) and evaluating the impact on cell viability, proliferation, and other pertinent outcomes [29].

# Assessment of cell viability and cytotoxicity induced by GMMP

To assess cytotoxicity, cells were initially seeded at a density of  $1\times10^4$  cells/ml in 96-well microtiter plates. Subsequently, after a 24 h incubation period, GMMP

was introduced at various concentrations (0.78, 1.56, 3.12, 6.25, 12.5, 25, and 50 µg/ml) and maintained for 24, 48, 72, and 96 h. The impact on cell viability was determined using the MTT assay following the standard protocol [30].

# Cell line groups and treatments

The cell lines used are CAOV-3 (representing ovarian cancer) and HEK-293 (representing normal kidney cells), which were classified according to the treatment as follows.

Control groups (G1 and G2): these groups serve as a baseline reference for HEK-293 and CAOV-3 cell line controls.

Negative control group (G3 and G4): the HEK-293 and CAOV-3 cells were treated with 100 µg/ml of GMMP.

Radiation groups (G5 and G6): the HEK-293 and CAOV-3 cells groups were treated with low-dose radiation (1.0 Gy of γ-irradiation) according to the protocol [30].

Combination groups (G7 and G8): the HEK-293 and CAOV-3 cell groups were exposed to 1.0 Gy of γ-irradiation and treated with 100 µg/ml of GMMP.

The samples of cells were collected after 96 h for further analysis. The measurements included BAX, BCL2, P53, MMP2, MMP9, caspase-3, and caspase-9 in HEK-293 and CAOV-3 cell lines after treatments.

# In-vivo study

# Induction of mice bearing solid tumor

Mammary adenocarcinoma cells (MACs) were utilized as a representative example of Ehrlich solid carcinoma in mice by injecting them into the right thigh of albino mice. The parent line will be donated from the National Cancer Institute (NCI), Cairo University. The preservation of the MAC cell line will be achieved through the intraperitoneal injection (IP) of 2.5 million cells per animal. Before IP injection, the MACs will be quantified using a bright-line hemocytometer and the dilution will be performed using a sterile physiological saline solution. A dose of  $0.2\,\mathrm{ml}$  containing  $2.5\!\times\!10^6\,\mathrm{MAC}$ s per animal will be subcutaneously (SC) injected into the right thigh of the female mouse's lower limb [31].

Mice radiation exposure and GMMP treatment protocol The radiotherapy regimen consisted of two stages for all mice with mice bearing solid tumor (MBST) or

treated with radiation alone or combined with GMMP. The radiation mice were exposed to γ-irradiation with two stages of exposure. In the first stage, the entire body was exposed to 0.5 Gy of γ-irradiation, then 30 min after this radiation dose, the first GMMP injection was given daily for 1 week. Then, the second stage started with another 0.5 Gy dose of γ-rays, after that the GMMP administration was resumed after 30 min for another 1 week, according to Nabil et al. [30].

# Experimental design

This study used 40 adult female Swiss albino female mice weighing about 20-25 g. The animals were categorized into five equal groups of eight mice as follows:

- Group (1), the control group (C): mice neither treated nor irradiated.
- Group (2): MBST.
- Group (3): MBST+GMMP: MBST were injected intraperitoneally daily with 100 mg/kg body weight from GMMP for 14 days starting from the first day after MAC inoculation.
- Group (4): including MBST and exposed for irradiation as the protocol above.
- Group (5): including MBST and exposed for irradiation as well as treated daily with 100 mg/kg body weight from GMMP for 14 days starting from the first day after MAC inoculation.

# Postexperimental procedures

Upon conclusion of the experimental period, the mice were killed using cervical dislocation, followed by necropsy procedures. Individual blood samples were collected from the inferior vena cava of MBST and collected plasma using heparin as an anticoagulant; after mixing for 10-20 min, centrifuge samples for 20 min at 3000 rpm for 15 min. The resultant plasma was preserved at -80°C until it was needed for further purposes. The tumors obtained from the left thigh muscles were processed for histological examination.

# Assessment of tumor weight and volume

After inoculating the tumor, the size of the left thigh in the lower limb of different experimental groups was determined using a digital electronic balance for weighing and a two-end electronic digital caliper from Switzerland for measuring. The measurements were conducted twice daily until the 28th day, signifying the end of the experiment. The size of the tumor was later determined using the formula outlined by Goto et al. [31]. The formula for calculating tumor

volume in cubic millimeters is follows:

Tumor Volume(mm<sup>3</sup>) = Length × (Width)<sup>2</sup>/2

# Measurement of biochemical parameters

Plasma levels of BAX, BCL2, P53, MMP2, MMP9, caspase-3, and caspase-9 were determined by ELISA, using commercially available kits of R & D Systems (USA) [32].

#### Statistical analysis

The collected data were coded, tabulated, and statistically analyzed using IBM SPSS statistics (Statistical Package for the Social Sciences) software version 28.0, IBM Corp., Chicago, Illinois, USA, 2021. Quantitative data were tested for normality using the Shapiro-Wilk test and then described as mean±SE. The groups were compared using a oneway analysis of variance, followed by Tukey's multiple comparison tests. The results will be deemed statistically significant if the *P* value is less than 0.05.

#### Results

# Isolation and identification of promising yeast highproducer pigment

The objective is to isolate and identify *Rhodotorula* mucilaginosa. Yeast isolates, named MMG and with an orange color, were obtained from a yogurt sample. The yeast isolate was orange-red when cultured on NA medium supplemented with 5% glycerol. The isolated yeast's pure culture was inspected under a microscope. The yeast obtained was oval and did not produce spores or form pseudo-true-mycelium. The 18 S rRNA gene was targeted by PCR to identify the possible R. mucilaginosa for further isolation. After that, partial sequencing was performed at Macrogen Com., Korea. Taxonomic identification of a selection of producing strains was performed with phylogenic analysis. Nucleotide sequences were compared with the GenBank databases using the BLASTN tool, which confirmed they belonged to R. mucilaginosa. The BLAST analysis revealed a complete similarity of 100% with R. mucilaginosa, so the GMM was identified as R. mucilaginosa GMM subsequently deposited in GenBank under accession number OQ120277. The phylogenetic tree was constructed using the 18 S rDNA sequence and the neighbor-joining technique (Fig. 1).

### **Production of pigment**

Isolation of the carotenoids of *R. mucilaginous* GMM cells was attempted using two different solvents in two extraction steps. The extraction yields expressed as grams of carotenoids extracted per gram of cells was 47.28%; the maximum extraction yield was 2.988 g/l and cell dry weight was 6.32 g/l. The results showed that the degree of pigmentation decreased with time, as did the pH, as the degree of pigmentation were 2.42, 2.2, and 2.07 at 24, 48, and 72 h, respectively, while pH was 3.76, 3.31, and 3.07, respectively.

#### **GMMP** characterization

The carotenoids' spectra were studied in the UV scanning to characterize the yeast pigment. The highest absorption level  $(\lambda_{\text{max}})$  was detected at a wavelength of 281 nm.

#### UPLC-ESI-qTOF-HRMS/MS profile of the GMMP

The LC-MS/MS processing was optimized with high efficacy for picking up and identifying 40 metabolites in R. mucilaginosa GMM, an orange pigment with

Figure 1

Rhodotorula mucilaginosa strain OP11 18S ribosomal RNA gene, partial sequence 🌳Rhodotorula mucilaginosa strain AUMC 10289 18S ribosomal RNA gene, partial sequence; internal transcribed spacer 1, 5.8S ribosomal RNA gene, and internal transcr... 🗣Rhodotorula mucilaginosa strain AUMC 8770 18S ribosomal RNA gene, partial sequence; internal transcribed spacer 1, 5.8S ribosomal RNA gene, and internal transcri... 🗣Rhodotorula mucilaginosa strain AUMC 9298 18S ribosomal RNA gene, partial sequence; internal transcribed spacer 1, 5.8S ribosomal RNA gene, and internal transcri... 🗣Rhodotorula mucilaginosa strain A86S2 internal transcribed spacer 1, partial sequence; 5.8S ribosomal RNA gene and internal transcribed spacer 2, complete sequence; ... 🖢 Agaricostilbomycetes sp. AYO-K04 internal transcribed spacer 1, partial sequence; 5.8S ribosomal RNA gene and internal transcribed spacer 2, complete sequence; and ... 🗣 Rhodotorula mucilaginosa isolate OMA Y14 internal transcribed spacer 1, partial sequence; 5.8S ribosomal RNA gene and internal transcribed spacer 2, complete seque... Rhodotorula mucilaginosa isolate L1Fa2-721 small subunit ribosomal RNA gene, partial sequence; internal transcribed spacer 1, 5.8S ribosomal RNA gene, and internal... Rhodotorula mucilaginosa isolate L1W1-713 small subunit ribosomal RNA gene, partial sequence; internal transcribed spacer 1, 5.8S ribosomal RNA gene, and internal ... 🖣 Rhodotorula mucilaginosa isolate K3F1-685 small subunit ribosomal RNA gene, partial sequence; internal transcribed spacer 1, 5.8S ribosomal RNA gene, and internal t... orula mucilaginosa isolate GMM internal transcribed spacer 1, partial sequence; 5.8S ribosomal RNA gene and internal transcribed spacer 2, complete sequence; ... 🕯 Rhodotorula mucilaginosa strain ATCC 74283 small subunit ribosomal RNA gene, partial sequence; internal transcribed spacer 1, 5.8S ribosomal RNA gene, and intern...

negative ion mode. The alignment of Rt values and monoisotopic masses for the molecular and some specific fragment ions and their relative abundances with the available scientific literature and the opensource software of a library database was used in the identification processes. Despite the identification of 40 individual metabolites (1-40), only five major corresponding broad peaks were recorded in each of the BPC chromatograms (Fig. 2a-c), which explains the co-elution of several compounds in each one; see Rt values in Table 1 and corresponding five MS1 spectra in Fig. 2dâ g, where each shows many [M-H] molecular ion peaks for a certain number of identified or unidentified metabolites. Accordingly, the number and area/s of the recorded five peaks cannot be computed as the correct measurable parameters for the actual number of the constitutive 40 metabolites (1-40) identified from R. mucilaginosa GMM orange pigment and their the concentrations. However, extracted MS chromatograms (XIC) and corresponding MS2 fragmentation spectra were essential in removing the corresponding peak area/s as a measurable parameter for the relative concentration and the tentative identification for the 40 metabolites (Table 1). The structures were established as eight tetra- (22, 26, 28, 35-39) and three triterpenoidal (23, 30, 33) carotenoids, six long-chain fatty acids (7, 21, 31, 32, 34, 40), nine organic acid derivatives (1, 2, 16, 18-20,

24, 27, 29), five amino acids (9, 11-14), four organic bases (3, 4, 15, 17), two sugars (5, 10), 2 polyhydric alcohols (6, 8), and a long-chain alkyl p-benzoquinones (25); their output MS data and chemical names are reported in Table 1 and structural formulas in Fig. 3.

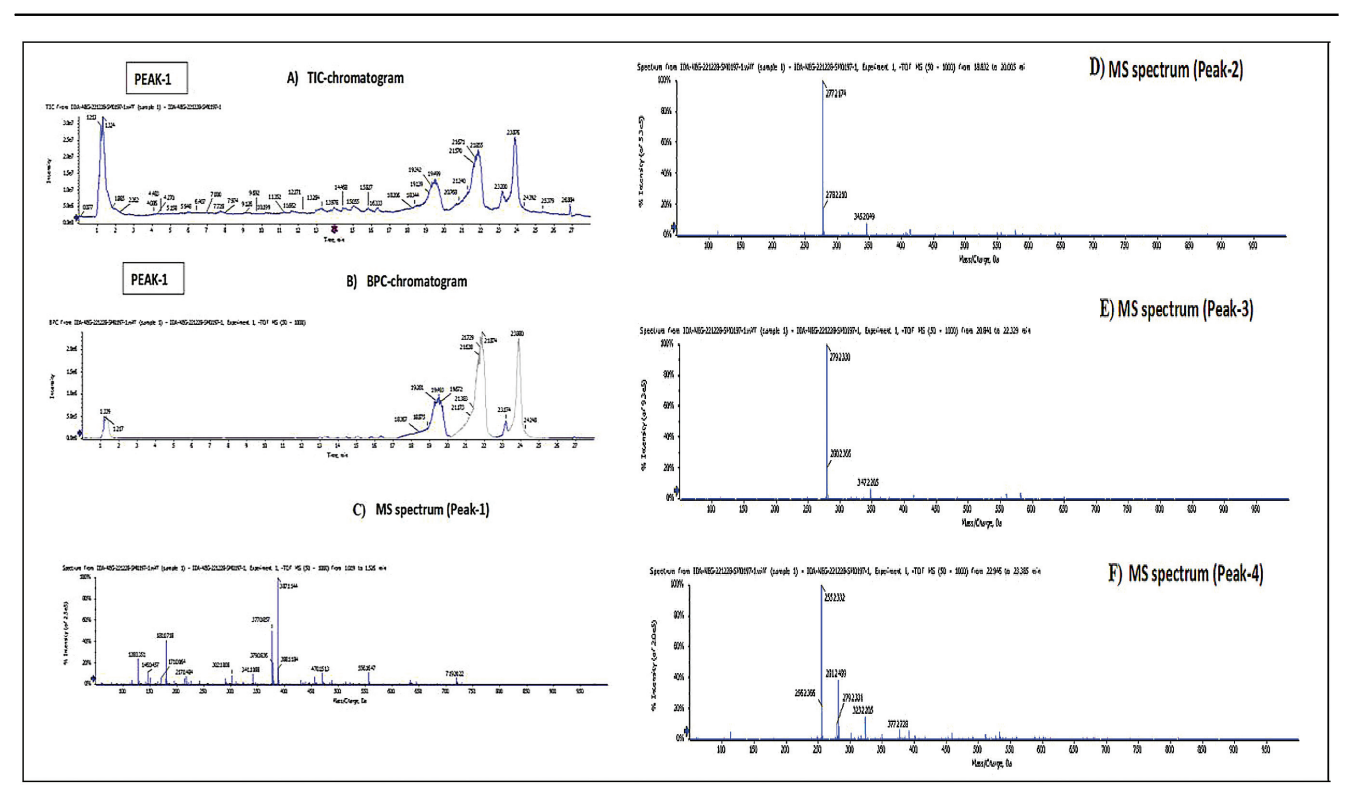
The LC-MS/MS analysis is performed on the partially extracted pigment depicted in Fig. 8. The liquid chromatogram signified the existence of distinct constituents, displaying the relative quantities of different chemicals being separated based on their retention time. A total of eight prominent carotenoid compounds have been identified through LC-MS analysis of the pigment produced by R. mucilaginosa GMM, including the carotenoids identified as Astraxanthin 4,4'-E-Diapophytoene, Torularhodin, 1,2,1',2'-Tetrahyroxylycopene, β-apo-8'-Carotenal, 10'-apo-E-β-caroten-10'-ol, 1,2,1',2'β-Carotene, Torulene, Echinenone, tetrahyroxydihydrolycopene, and α-Canthaxanthin at a retention time of 13.490, 13.940, 15.830, 16.190, 16.470, 20.870, 22.174, 23.179, 23.182, 23.189, and 23.779 min, respectively.

#### In-vitro result

# Antioxidant activity using DPPH

The ability of various concentrations of the yeast pigment (GMMP) to scavenge free radicals was evaluated. The results showed that the purified





(a-g) MS spectra fragment of different carotenoids isolated by LC-MS. LC-MS, liquid chromatography-mass spectrometric.

$\overline{}$
뿆
×
×
⊏
a
×
€.
ᇴ
Ö
ď
č
TOF-HRMS/MS (r
'n
¥
≥
'n.
⋍
2
Œ
I
.7
뽀
0
Η.
℧
I
nent by LC/ESI
űί
=
O
Į.
_
≥
7
<u>.</u>
Ē
Ō
⊱
ᇑ
.≚′
Ω.
MMG
≤
Σ
否
U
æ
ľĀ
٠,
ő
ő
yinos
aginos
laginos
cilaginos
ucilaginos
nucilaginos
mucilaginos
a mucilaginos
ıla mucilagino
rula mucilaginos
orula mucilaginos
torula mucilaginos
otorula mucilaginos
dotorula mucilaginos
odotorula mucilaginos
hodotorula mucilaginos
Rhodotorula mucilaginos
n Rhodotorula mucilaginos
m <i>Rhodotorula mucilagino</i> s
om Rhodotorula mucilaginos
rom <i>Rhodotorula mucilagino</i> s
from Rhodotorula mucilaginos
d from <i>Rhodotorula mucilagino</i> s
ed from Rhodotorula mucilaginos
fied from Rhodotorula mucilaginos
tified from <i>Rhodotorula mucilagino</i> s
ntified from Rhodotorula mucilaginos
entified from <i>Rhodotorula mucilagino</i> s
dentified from Rhodotorula mucilaginos
identified from Rhodotorula mucilaginos
<ol> <li>identified from Rhodotorula mucilaginos</li> </ol>
40) identified from Rhodotorula mucilaginos
40) identified from Rhodotorula mucilaginos
1–40) identified from Rhodotorula mucilaginos
(1–40) identified from Rhodotorula mucilaginos
s (1–40) identified from <i>Rhodotorula mucilagino</i> s
es (1–40) identified from Rhodotorula mucilaginos
ites (1–40) identified from <i>Rhodotorula mucilagino</i> s
olites (1–40) identified from <i>Rhodotorula mucilagino</i> s
oolites (1–40) identified from Rhodotorula mucilaginos
bolites (1–40) identified from <i>Rhodotorula mucilagino</i> s
tabolites (1–40) identified from <i>Rhodotorula mucilagino</i> s
etabolites (1–40) identified from Rhodotorula mucilaginos
Wetabolites (1–40) identified from Rhodotorula mucilaginos
Metabolites (1–40) identified from Rhodotorula mucilaginos
1 Metabolites (1–40) identified from Rhodotorula mucilaginos
1 Metabolites (1-40) identifi
ble 1 Metabolites (1–40) identified from Rhodotorula mucilaginos

					æ																, 20)				oxo- ran-9-	
Chemical Name		Succinic acid (1)	(S)-Malic acid (2)	Uridine-5-monophosphate (3)	2'-Deoxyguanosine 5'- Monophosphate (4)	D-Fructose (5)	Ribitol (6)	Azelaic acid (7)	Mannitol (8)	N-Acetyl-L-leucine (9)	Sucrose (10)	5-Oxo-D-proline (Pyroglutamic acid, 11)	L-Norvaline (12)	DL-Norleucine (13)	L-Isoleucine (14)	Adenine (15)	$\alpha$ -Ketoadipic acid (16)	Diuron(17)	Gallic acid (18)	Vanillin (19)	2,4,5-Trimethoxybenzoic acid (Asaronic acid, 20)	Palmitic acid (21)	Astraxanthin (22)	4,4'-E-Diapophytoene (23)	4-Hydroxy-4-(hydroxymethyl)-6,7-dimethyl-3-oxo-1,3,4,7, 7a,9a- hexahydropentaleno[1,6a-c]pyran-9-carboxylic acid (24)	
Area		1658319	313575	1015160	738720	2764499	2533762	604681	18825672	28504	2620842	8537783	730424	1286057	1514467	1502030	26240	11349	46710	16495	62132	10051	144247	387087	1447615	462930
MS/MS Fragments		55.019, 71.012, 73.029, 81.292 99.004, 117.019	71.011, 89.023, 89.048, 115.005, 133.012	78.957, 96.969, 111.019,120.969, 132.030, 138.983, 171.007, 210.323, 211.000, 212.004, 280.02344, 305.075, 323.025	78.958, 96.970, 128.030, 129.016, 134.045, 168.023, 192.989, 195.046, 210.998, 309.976, 346.051, 1962	59.01356, 71.01256, 83.01358, 85.02903, 89.02184, 97.02893, 103.03532,115.04629,131.03622,161.04112, 179.05246	55.(	58.02933, 97.0664, 123.07636, 124.70165, 125.09305, 169.07603, 187.06914, 187.10004	55.01981, 57. 83.01248, 113.0242, 1	72.0049, 88.04117, 104.03682, 130.09058, 172.09734	÷	72.00614, 82.02835, 127.62992, 128.03548	99.92829, 116.06631	58.03152, 71.0149, 130.08887	86.99256, 130.07487, 130.08775	65.01508, 68.02451, 92.02628, 107.03574, 134.04741	59.01381, 70.99974, 114.98907, 115.98767, 130.98647, 158.97826, 159.05305	68.99927, 104.95364, 129.00093, 134.03256 151.0575, 203.05991, 231.09058	125.09371, 169.08412	79.9824, 92.02511, 108.01999, 136.0201, 151.03702	102.95552, 116.0441, 140.04024, 140.05194, 167.0592, 211.08511	102.95554, 112.98548, 170.94389, 186.93282, 255.234	152.9943, 241.0104, 279.2330, 315.0476, 595.2849	78.9550, 152.9943, 283.9384, 407.2171	113.08714, 149.09225, 171.09853, 179.12057, 185.117, 195.1395, 221.15704, 249.23009, 275.18835, 293.21536	79 95841 96 95700 221 15533 292 23239 293 17947
: <b>I</b>		118.0266	134.0215	324.0359	347.0631	180.0634	152.0685	188.1049	182.0790	173.1052	342.1162	129.0426	117.0790	131.0946	131.0946	135.0545	160.0372	232.0170	170.0215	152.0474	212.0685	256.2402	596.3865	408.3756	294.1104	1001
[MH] <sub>cal</sub> Error, MF MW		$C_4H_6O_4$	$C_4H_6O_5$	C <sub>9</sub> H <sub>13</sub> N2O <sub>9</sub> P	$C_{10}H_{14}N_5O_7P$	$C_6H_{12}O_6$	C <sub>5</sub> H1 <sub>2</sub> O <sub>5</sub>	$C_9H_{16}O_4$	C <sub>6</sub> H <sub>14</sub> O <sub>6</sub>	C <sub>8</sub> H <sub>15</sub> NO <sub>3</sub>	C <sub>12</sub> H <sub>22</sub> O <sub>11</sub>	$C_5H_7NO_3$	$C_5H_{11}NO_2$	$C_6H_{13}NO_2$	$C_6H_{13}NO_2$	$C_5H_5N_5$	$C_6H_8O_5$	$C_9H_{10}CI_2N_2O$	C <sub>7</sub> H <sub>6</sub> O <sub>5</sub>	$C_8H_8O_3$	$C_{10}H_{12}O_5$	$C_{16}H_{32}O_{2}$	$C_{40}H_{52}O_4$	$C_{30}H_{48}$	C <sub>15</sub> H <sub>18</sub> O <sub>6</sub>	T.
Error,	mdd	0.5	0.2	9.6	9.0	4.6	-0.2	5.6	1.3	4.1-	<del>1</del> .	8.5	-2.4	11.2	7.3	0.8	4	1.8	0.3	4.1	6.0-	3.6	4.0	0.22	3.6	0.1
[MH] <sub>cal</sub>		117.0193	133.0143	323.0286	346.0558	179.0561	151.0612	187.0976	181.0718	172.0979	341.1089	128.0353	116.0717	130.0874	130.0874	134.0472	159.0299	231.0097	169.0143	151.0401	211.0612	255.2330	595.3787	407.3678	293.1030	293.1758
sqo [HM]		117.018	133.014	323.025	346.055	179.0549	151.060	187.096	181.071	172.062	341.107	128.033	116.071	130.085	130.085	134.047	159.101	231.087	169.087	151.038	211.088	255.231	595.284	407.288	293.211	293,179
P.		1.059	1.097	1.097	1.123	1.123	1.287	1.299	1.324	1.324	1.324	1.350	1.388	1.401	1.640	1.730	4.676	5.059	5.961	8.295	10.460	12.175	13.490	13.940	14.047	15 150
		119	295	320	533	202	1199	1257	1786	1784	1798	558	2254	2309	2777	2813	2923	2942	2995	3200	3285	3384	3987	3981	3585	3787

Table	Table 1 (Continued)	(penu							
Q	$R_t$	[MH] obs	$[MH]_{cal}$	Error, ppm	MF	MM	MS/MS Fragments	Area	Chemical Name
									2,5-Dihydroxy-3-undecylcyclohexa- 2,5-diene-1,4- dione (Embelin, 25)
4979	15.830	563.3159	563.3889	0.3	$C_40H_{52}O_2$	564.3967	152.9953, 278.2198, 503.2942, 563.3159	11446675	Torularhodin(26)
3943	16.168	485.282	485.3272	-0.3	C <sub>30</sub> H <sub>46</sub> O <sub>5</sub>	486.3345	112.97935, 180.96838, 180.9874, 248.95177, 248.9807, 265.13828, 280.11365, 286.93094, 288.95825, 316.965, 332.91757, 348.90543, 354.92172, 400.88672, 428.218, 439.28607, 455.212, 469.2486, 483.69006, 483.70871, 485.27536	263819	(1 R,2 S,5aR,5bR,7aS,10 R,12bR)-2- Hydroxy-10-isopropenyl 3.3,5a,5b, 12b-pentam Ethyloctadecahydro dicyclopenta [a, i]phenanthrene-1,7a(1H)-dicarboxylic acid (27)
5253	16.190	599.324	599.4001	0.32	$C_{40}H_{56}O_4$	600.4179	152.9917, 283.2648, 419.2478, 599.3258	279114	1,2,1',2'-Tetrahyroxylycopene (28)
3956	16.305	339.196	339.1602	8. S.	C <sub>21</sub> H <sub>24</sub> O <sub>4</sub>	340.1675	79.95741, 102.96004, 119.04981, 155.98367, 170.0092, 182.99007, 183.01299, 184.01927, 197.02875, 198.035, 215.99048, 216.00916, 225.06647, 270.89081, 275.247, 338.0759, 338.10706, 339.16995, 339.19595	425838	2-Hydroxy-4-methoxy-3-(3-methyl but-2-enyl)-6-(2- phenylethyl)benzoic acid (Amorfrutin 1, 29)
5340	16.470	415.317	415.3001	-1.1	$C_{30}H_{40}O$	416.3079	102.9569, 210.9203, 346.8940, 415.2929	298600	E-β-apo-8'-Carotenal (30)
4096	18.264	277.216	277.2173	1.7	C <sub>18</sub> H <sub>30</sub> O <sub>2</sub>	278.2246	59.01198, 71.0132, 127.06973, 127.08247, 233.22597, 258.36926, 259.19846, 275.19156, 275.21265, 276.331, 276.37823, 277.21701	3135818	Linolenic acid (31)
4361	20.611	253.218	253.2173	-2.4	C <sub>16</sub> H <sub>30</sub> O <sub>2</sub>	254.2246	225.06892, 252.4003, 253.21762	1490630	Palmitoleic acid (32)
7820	20.870	377.308	377.2844	1.9	$C_{27}H_{38}O$	378.2923	104.9506, 240.9198, 309.2001, 377.2001	214015	10'-apo- E-β-caroten-10'-ol (33)
4595	22.072	279.257	279.2329	-85.9	C <sub>18</sub> H <sub>32</sub> O <sub>2</sub>	280.2402	59.01107, 83.050, 97.06879, 127.074, 233.22, 243.201, 259.21457, 261.19641, 261.22153, 278.332, 279.14862, 279.2312	1078769	9Z,12Z-Octadecadienoic acid (Linoleic acid, 34)
8706	22.174	535.470	535.4304	- <del>3</del> .1	$C_{40}H_{56}$	536.4382	255.2340, 279.2325, 535.3754		β-Carotene (35)
4829	23.179	533.451	533.4147	0.45	$C_{40}H_{54}$	534.4226	102.9621, 255.2331, 313.1730, 381.1818, 533.4562	471733	Torulene (36)
9492	23.182	549.429	549.4096	0.42	$C_{40}H_{54}O$	550.4175	255.2324, 409.3097, 549.4298	180607	Echinenone (37)
4856	23.189	601.441	601.4257	-0.1	$C_{40}H_{58}O_4$	602.4335	255.2318, 323.2198, 533.4562, 601.4380	409301	1,2,1',2'-Tetrahyroxydihydrolycopene (38)
5283	23.779	563.499	563.3889 563.4996	0.5	$C_{40}H_{52}O_{2}$	564.3967	281.25024, 563.41101, 563.50488	306983	$\alpha$ -Canthaxanthin (39)
5120	23.884	281.249	281.2486	-2.5	C <sub>18</sub> H <sub>34</sub> O <sub>2</sub>	282.2559	97.0684, 127.07266, 263.2493, 279.71921, 280.34546, 281.09787, 281.13577, 281.24942	247297808	n-Undecylic acid (Elaidic acid, 40)

HO OH	HO OH OH 2	O O OPO(OH) <sub>2</sub> OHO OHO	HOOH OH 5	HO OH OH OH
OH O O OH	HO OH OH	PO HN HN HO	HO OH HO OH	OH OH
OH NH <sub>2</sub> 12	OH NH <sub>2</sub> 13	OH NH <sub>2</sub> 14	NH <sub>2</sub> HN N	HO 0 OH
O H CI	O OH HO OH OH OH 18	0 19	O O H	OH OOH 25
O <sub>OH</sub> 21	<b>~~~</b>	HOOH	28	- HO НО
35		HO OH HO 24	HO, OPO(OH)2	HO OH OH
	26	ОН	30	

Structural formula of different carotenoids in natural pigment.

GMMP exhibited scavenging activity toward DPPH radicals in a concentration-dependent manner. The reduction was increased with increasing time exposure and concentration of pigment, with an IC<sub>50</sub> value of 4 mg/ml. Figure 4 shows the highest DPPH scavenging activities were 95.71 at 10 mg/ml. The results showed good antioxidant activity at 10 mg/ml yeast pigment exhibiting a percentage inhibition of 95.71% radical scavenging activity after 120 min.

# Antioxidant activity of GMMP as assessed by the oxygen radical scavenging capacity assay

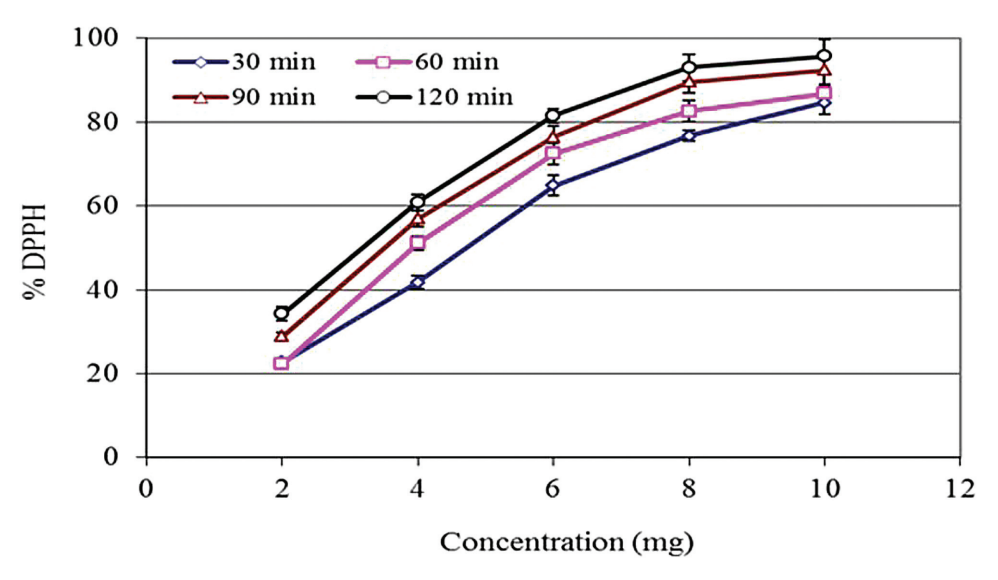
The antioxidant activity of GMMP using the oxygen radical scavenging capacity (ORAC) assay revealed that GMMP exhibited a substantial antioxidant capacity, with an ORAC value of 1 610 991  $\mu$ M Trolox equivalents (TE) TE/mg sample. The standard deviation for this measurement was 315.42  $\mu$ M TE/mg sample, indicating the reliability and consistency of GMMP's antioxidant activity (Fig. 5a–c).

# MTT test in Caov-3 and HeK-293 cell lines after radiation exposure and treated with GMMP

CAOV-3 cells were much less alive after being treated with a mix of GMMP and low-dose radiation

compared with cells that had not been treated (P<0.001) (Fig. 6a-c). To assess its anticancer impact, we investigated a CAOV-3 treated with GMMP at concentrations of 0.78, 1.56, 3.12, 6.25, 12.5, 25, and 50 µg/ml. The MTT test showed that GMMP strongly inhibited CAOV-3 after 24, 48, or 96 h of treatment (Fig. 6). The cytotoxicity of GMMP extract was evaluated at a dose of 50 µg/ml against CAOV-3 (Fig. 6). The results indicated that GMMP was highly effective against the CAOV-3, with an IC<sub>50</sub> value of 0.697 μmol/ml (Fig. 6a). We found out how GMMP affected the viability of the CAOV-3 and HEK-293 by measuring its cytotoxic effect at different concentrations (0.78, 1.56, 3.12, 6.25, 12.5, 25, and 50 µmol/ml). Doxorubicin, an anticancer drug, is a positive control. The results showed that the viability of CAOV-3 and HEk-293 was reduced gradually as concentrations of GMMP doxorubicin increased. With CAOV-3, the IC<sub>50</sub> of GMMP was 0.697 µmol/ml, while doxorubicin was 7.65  $\mu$ mol/ml. In HEK-293 cells, the IC<sub>50</sub> was 1127 µg/ml and 386.15 µg/ml for GMMP and doxorubicin, respectively, as represented in Fig. 6b and c. The IC<sub>50</sub> of GMMP on CAOV-3 in the presence of radiation was 0.22 µmol/ml, while on

Figure 4



DPPH scavenging activity of GMMP.

HEK-293 in the presence of radiation was 0.345 μmol/

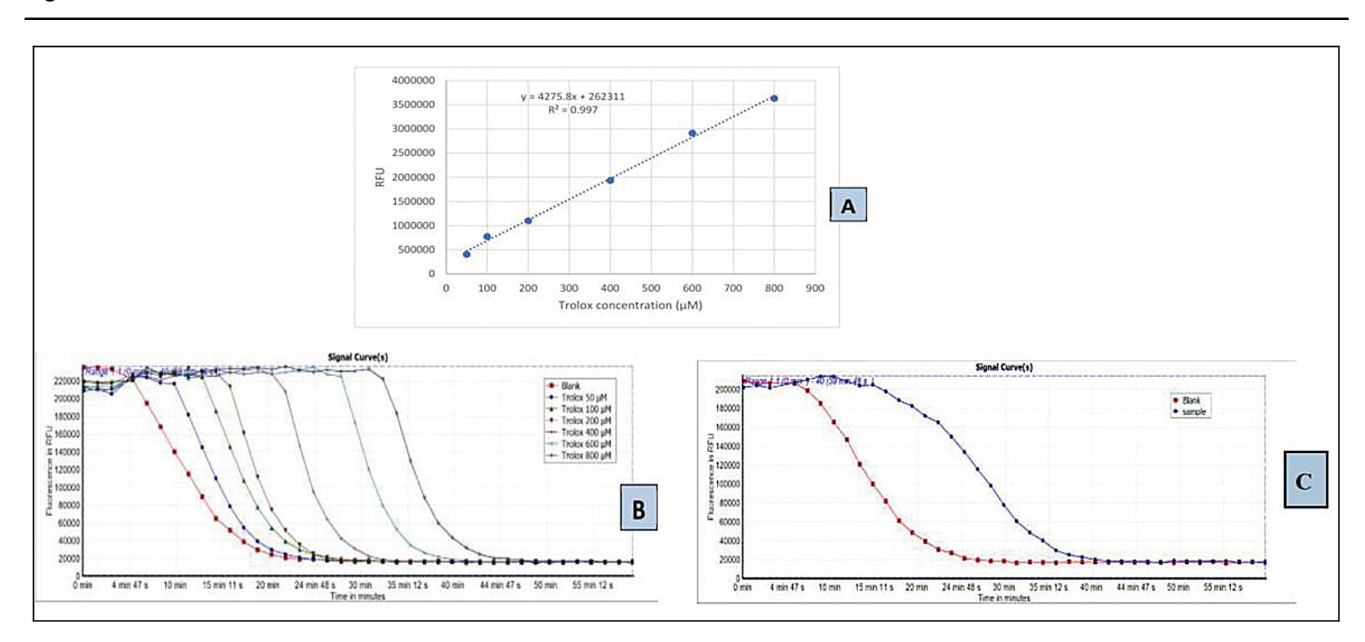
#### BAX and Bcl2 expression

The proapoptotic marker BAX and the antiapoptotic marker Bcl2 were evaluated (Table 2). BAX levels were significantly increased (P=0.001) in the CAOV-3 treated with GMMP and CAOV-3 treated with GMMP and exposed to radiation groups (1.23) ±0.02) and (1.47±0.022), respectively, while BCL2 levels were significantly decreased in the CAOV-3 treated with GMMP and/or treated with GMMP and exposed to radiation groups (Table 2).

#### P53 expression

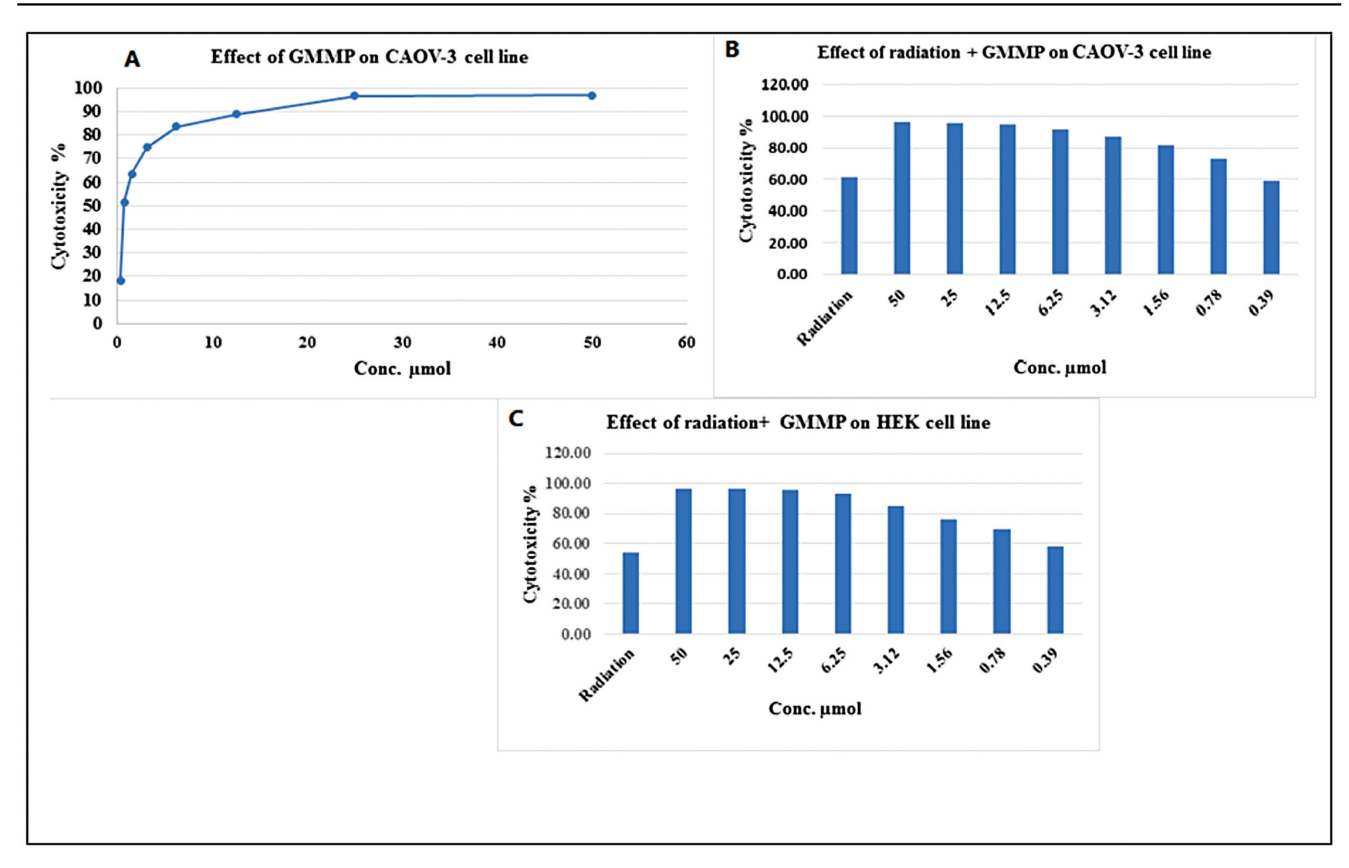
The tumor suppressor gene P53 showed variations in expression across groups (Table 2). Treatment of CAOV-3 with GMMP alone increased the p53 level to 2.21±0.030 pg/mg. In these cells, the combination of GMMP and radiation further elevated the p53 level to 2.80±0.022 pg/mg in the Caov-3 cells.

Figure 5



Trolox exhibits an antioxidant impact on the degradation of fluorescein in the ORAC assay: (a) Corrected linear regression curve for Trolox. (b) The signal curve for different Trolox concentrations and a blank sample show how fluorescein breaks down at different Trolox concentrations. (c) The signal curve of the samples and blank demonstrates the decline of fluorescein with cell culture application.

Figure 6



MTT test in CAOV-3 and HEK293 cell lines after radiation exposure and treated with GMMP: (a) Cytotoxicity of GMMP on CAOV-3 cell lines, (b) the effect of radiation exposure and treated with GMMP on CAOV-3, (c) the effect of radiation exposure and treated with GMMP on HEK293 cell lines.

# MMP2 and MMP9 levels

MMP2 and MMP9 levels indicated variations across treatment groups. In the CAOV-3 cells, GMMP treatment alone or in combination with radiation reduced MMP2 and MMP9 levels compared with untreated controls (Table 2).

# Caspase-3 and caspase-9 levels

Significant changes were seen in the levels of both caspase-3 and caspase-9 among the different treatment groups (Table 2). The CAOV-3 treated with GMMP and GMMP with radiation exhibited a significant increase of caspase-3 and caspase-9 when compared with untreated cells.

#### In-vivo result

Biological marker evaluation in mice bearing solid tumor after radiation exposure and treated with GMMP

Tumor size: Changes in tumor diameter (TD) were assessed in different groups over 28 days following the injection of MBST (Fig. 7). At the end of the trial, (Figure 7) clearly showed that those in the treatment groups (MBST treated with GMMP; MBST exposed to radiation; and MBST treated with GMMP and

exposed to radiation) had significantly less tumor weight and volume than those who did not receive MBST treatment. The dual treatment group had the highest reduction ratio compared with the MBST treated by GMMP and Rad therapy group.

#### BAX and Bcl2 levels

The proapoptotic protein BAX and the antiapoptotic protein Bcl2 levels were evaluated across different experimental groups (Table 3). The MBST without treatments showed a decrease in BAX level (0.15 ±0.003 pg/mg) and an increase in Bcl2 level (1.7 ±0.03 pg/mg) compared with the control. Radiation treatment alone in MBST led to a further increase in BAX (1.33±0.02 pg/mg) and a decrease in Bcl2 (0.37 ±0.04 pg/mg), suggesting a shift toward a proapoptotic state. Treatment with GMMP alone in MBST resulted in a substantial elevation of BAX (1.80  $\pm 0.04 \,\mathrm{pg/mg}$ ) and a reduction in Bcl2 (0.26 $\pm 0.02 \,\mathrm{pg/mg}$ ) mg). The combination of GMMP and radiation in MBST exhibited the highest BAX level (1.97±0.06 pg/ mg) and a moderately increased Bcl2 level (0.33 ±0.02 pg/mg) compared with the GMMP- alone group.

Table 2 BAX, BCL2, P53, MMP2, MMP9, caspase-3, and caspase-9 levels in Caov-3 and HeK-293 cell lines after radiation exposure and treated with natural pigment

	HeK-293 (G1)	Caov-3 (G2)	HeK-293+ GMMP (G3)	CAOV-3+ GMMP (G4)	HeK-293+ Rad. (G5)	CAOV-3+ Rad. (G6)	HeK-293+ GMMP +Rad. (G7)	CAOV-3+GMMP + Rad. (G8)
BAX (pg/mg)	0.32±0.016 <sup>f</sup>	0.48±0.027 <sup>de</sup>	0.39±0.028 <sup>ef</sup>	1.23±0.020 <sup>b</sup>	0.53±0.016 <sup>d</sup>	0.8±0.017°	0.33±0.014 <sup>†</sup>	1.47±0.022ª
BCL2 (pg/mg)	0.83±0.013 <sup>b</sup>	$1.01\pm0.015^{a}$	1.00±0.016 <sup>a</sup>	0.21±0.014 <sup>de</sup>	$0.33\pm0.014^{\circ}$	$0.27\pm0.012^{cd}$	$0.96\pm0.014^{a}$	0.18±0.014 <sup>e</sup>
P53 (pg/mg)	$0.55\pm0.014^{\text{de}}$	$0.54\pm0.014^{\text{de}}$	0.50±0.014 <sup>e</sup>	2.21±0.030 <sup>b</sup>	0.57±0.014 <sup>d</sup>	1.40±0.020°	$0.59\pm0.014^{d}$	2.80±0.022 a
MMP2 (pg/mg)	0.187±0.005 <sup>bc</sup>	1.90±0.023ª	0.2±0.006 <sup>b</sup>	0.20±0.006 <sup>b</sup>	0.19±0.003 <sup>bc</sup>	0.23±0.009 <sup>b</sup>	0.23±0.011 <sup>b</sup>	$0.15\pm0.005^{c}$
MMP9 (pg/mg)	0.30±0.013 <sup>bc</sup>	0.40±0.011 <sup>a</sup>	0.30±0.009 <sup>bc</sup>	0.21±0.011 <sup>d</sup>	0.27±0.011°	0.34±0.011 <sup>b</sup>	0.27±0.011°	0.19±0.011 <sup>d</sup>
Caspase-3 (ng/mg)	$6.67\pm0.060^{\dagger}$	7.70±0.071 <sup>e</sup>	7.70±0.071 <sup>e</sup>	20.33±0.090 b	6.68±0.063 <sup>f</sup>	17.70±0.071°	9.70±0.071 <sup>d</sup>	23.01±0.073 a
Caspase-9 (ng/mg)	$6.58\pm0.062^{d}$	9.10±0.071°	7.00±0.071 <sup>d</sup>	20.33±0.090 a	7.03±0.310 <sup>d</sup>	18.27±0.092 <sup>b</sup>	6.70±0.071 <sup>d</sup>	20.70±0.071 <sup>a</sup>

alue figment; Rad, radiation exposure. All data are expressed as mean±SE. Values in the same row with the different superscript letters (a, b, c, d, e, f) are significantly different at P value ess than 0.05, using one-way analysis of variance and then Tukey's post-hoc comparison

### P53, MMP2, and MMP9 levels

The tumor suppressor protein p53 levels were evaluated across different experimental groups (Table 3). In the control group, the p53 level was 0.33±0.011 pg/mg. The MBST without treatments exhibited a higher p53 level of 0.80±0.012 pg/mg than the control. Radiation treatment in MBST significantly increased p53, reaching 1.40±0.021 pg/mg. Interestingly, treatment with GMMP alone in MBST also resulted in a p53 level of 1.40±0.02 pg/mg, similar to the radiationgroup. However, the combination of and radiation in MBST **GMMP** showed a synergistic effect, with the highest p53 level 1.80±0.022 pg/mg. observed The metalloproteinases MMP2 and MMP9 levels were evaluated across the different experimental groups. In the control group, the MMP2 level was 0.27 ±0.004 pg/mg, and the MMP9 level was 0.17 ±0.002 pg/mg. The MBST without treatments exhibited significantly higher levels of both MMP2  $(0.77\pm0.004 \,\mathrm{pg/mg})$  and MMP9  $(0.43\pm0.02 \,\mathrm{pg/mg})$ compared with the control. Interestingly, treatment with GMMP alone in MBST decreased MMP2  $(0.20\pm0.003 \,\mathrm{pg/mg})$  and MMP9  $(0.20\pm0.02 \,\mathrm{pg/mg})$ levels compared with the untreated MBST. The combination of GMMP and radiation in MBST also showed a reduction in MMP2 (0.23±0.003 pg/ mg) and MMP9 (0.17±0.003 pg/mg) levels, with the MMP9 level being similar to the control group.

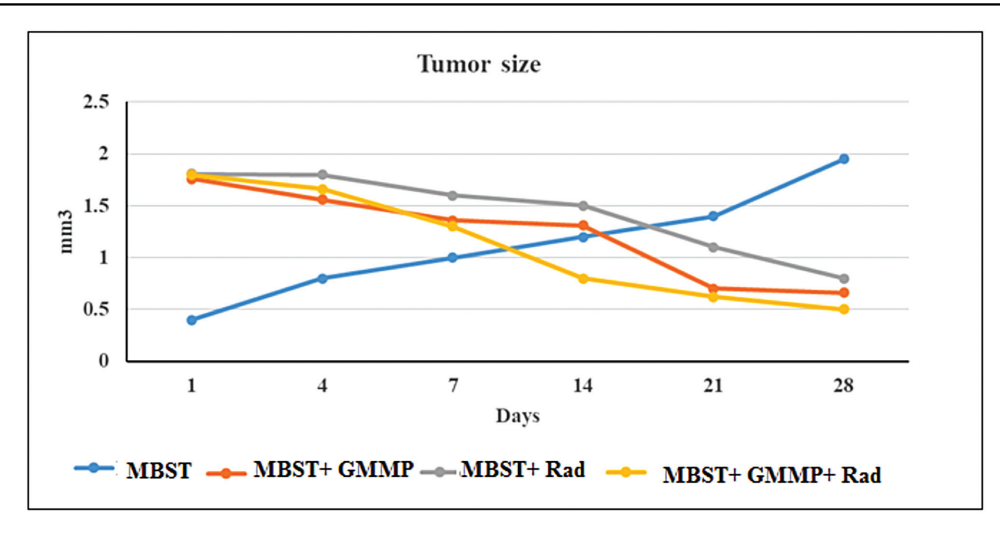
# Caspases-3 and 9

The levels of the apoptosis-executing enzyme caspase-3 and the initiator caspase-9 were evaluated in the different experimental groups (Table 3). In the control group, the caspase-3 level was 2.70±0.04 ng/mg, and the caspase-9 level was 4.33±0.32 ng/mg. treatment with GMMP alone in MBST resulted in elevated levels of caspase-3 (10.34 ±0.30 ng/mg) and caspase-9 (18.34±0.44 ng/mg). Radiation treatment alone in MBST significantly increased caspase-3 (7.33±0.32 ng/mg) and caspase-9 (17.68±0.32 ng/mg) levels. Notably, the combination of GMMP and radiation in MBST exhibited a synergistic effect, with the highest levels of caspase-3 (13.02±0.76 ng/mg) and caspase-9 (20.02±0.88 ng/ mg) observed among all groups (Table 3).

# Histopathological findings

Microscopical examination of the skeletal muscle tissue section of the normal control group revealed small bundles of muscle fibers, and each bundle is separated by a connective tissue layer called Another thin layer of reticular perimysium. connective tissue fiber called endomysium invests the

Figure 7



The tumor size in female mice bearing solid tumors after being treated with natural pigment alone or with radiation exposure.

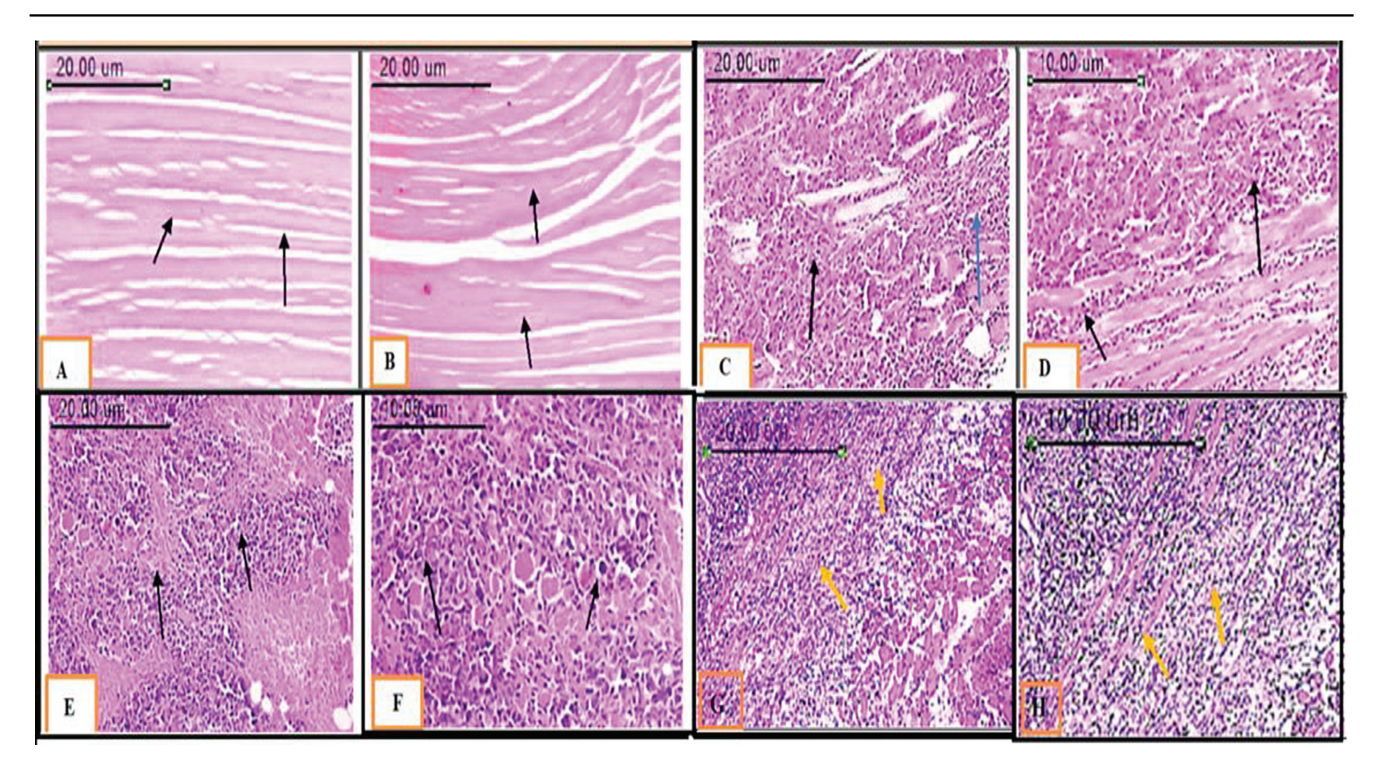
Table 3 BAX, BCL2, P53, MMP2, MMP9, caspase-3, and caspase-9 levels in female mice bearing solid tumor after radiation exposure and treated with natural pigment

-					
	Control (Group 1)	MBST (Group 2)	MBST+GMMP (Group 3)	MBST+Rad (Group 4)	MBST+Rad+GMMP (Group 5)
BAX (pg/mg)	0.43±0.010 <sup>d</sup>	0.15±0.003 <sup>e</sup>	1.80±0.04 <sup>b</sup>	1.33±0.020 <sup>c</sup>	1.97±0.060 <sup>a</sup>
BCL2 (pg/mg)	0.73±0.020 <sup>b</sup>	1.70±0.030 <sup>a</sup>	0.26±0.02 <sup>e</sup>	0.37±0.040 <sup>c</sup>	0.33±0.02 <sup>d</sup>
P53 (pg/mg)	0.80±0.012 <sup>c</sup>	0.33±0.011 <sup>d</sup>	1.40±0.022 <sup>b</sup>	1.40±0.020 <sup>b</sup>	1.80±0.022 <sup>a</sup>
MMP2 (pg/mg)	0.27±0.004 <sup>c</sup>	0.77±0.004 <sup>a</sup>	0.20±0.003 <sup>e</sup>	0.30±0.004 <sup>b</sup>	0.23±0.003 <sup>d</sup>
MMP9 (pg/mg)	0.17±0.002 <sup>c</sup>	0.43±0.020 <sup>a</sup>	0.20±0.02 <sup>c</sup>	0.27±0.030 <sup>b</sup>	0.17±0.003 <sup>c</sup>
Caspase-3 (ng/mg)	3.01±0.040 <sup>d</sup>	2.70±0.040 <sup>e</sup>	10.34±0.30 <sup>b</sup>	7.33±0.320 <sup>c</sup>	13.02±0.76 <sup>a</sup>
Caspase-9 (ng/mg)	5.70±0.210 <sup>d</sup>	4.33±0.320 <sup>e</sup>	18.34±0.44 <sup>b</sup>	17.68±0.320 <sup>c</sup>	20.02±0.88 <sup>a</sup>

GMMP, natural pigment; MBST, mice bearing solid tumor; Rad, radiation exposure. All data are expressed as mean±SE. Values in the same row with the different superscript letters (a, b, c, d, e) are significantly different at *P* value less than 0.05, using one-way analysis of variance and then Tukey's post-hoc comparison.

individual muscle fiber (Fig. 8a and b). The histopathological analysis of the solid tumor in the animal group revealed a dense accumulation of tumor cells that had infiltrated both the muscular and subcutaneous tissues. The Ehrlich tumor cells are organized in clusters or sheets, displaying profoundly pleomorphic nuclei basophilic with vesicularity. The solid tumor comprises polygonal exhibit pleomorphic morphologies, hyperchromatic nuclei, and anisocytosis. A modest quantity of recently developed blood capillaries (neovascularization) was observed in the adjacent tissue (Fig. 8c and d). In addition, a few instances of fibrous tissue growth were observed (Fig. 8 and Table 4). Upon microscopic analysis of the skeletal muscle tissue section from the standard control group, it was observed that the muscle fibers were arranged in little bundles. A layer of connective tissue known as the perimysium separates these bundles. Endomysium, a thin reticular connective tissue fiber layer, surrounds each muscle fiber (Fig. 8a and b). The animal group's solid tumor was looked at using histopathology, which showed a dense collection of tumor cells that had spread into the muscle and subcutaneous tissues. Ehrlich tumor cells are arranged in sheets or clusters, and their nuclei are deeply basophilic and pleomorphic, with nuclear vesicularity. The tumor comprised polygonal cells with pleomorphic morphologies, hyperchromatic nuclei, anisocytosis. The tissue sections of solid tumors in animals treated with GMMP or Rad showed degenerative alterations characterized by vacuolation of neoplastic cells (Fig. 8e and f). The Ehrlich tumor cells exhibited significant pyknosis and karyolysis, particularly in the central portions of the tumors (Fig. 8g). Many inflammatory cells, primarily lymphocytes, macrophages, and multinucleated tumor giant cells, infiltrated the necrotic regions. However, only a small amount of fibrous tissue growth was observed (Fig. 8h and Table 4). The

Figure 8



Tissue section of Ehrlich solid tumor showing: (a and b) normal skeletal muscle tissue section showed bundles of muscle fibers, and each bundle is separated by a connective tissue layer arrow (20.00 µm); (c) aggregation of carcinoma cells that invade muscular and subcutaneous tissues arrow (20.00 μm); (d) sheet of deeply basophilic polygonal cells with hyperchromatic nuclei arrow (10.00 μm); (e) compact aggregation of tumor tissue cells within the muscular and subcutaneous tissues arrow (20.00 µm); (f) tumor cells arranged in the form of clusters with deeply basophilic pleomorphic nuclei arrow (10.00 μm); (g) marked proliferation of fibrotic tissues with intense leukocyte infiltration arrow (20.00 μm); (h) pyknosis and karyolysis of Ehrlich tumor cells arrow (10.00 µm).

exhibited considerable surrounding tissue neovascularization, as observed in Fig. 8g and h.

#### **Discussion**

The findings align with the study conducted by Kanzy et al. [33], which involved the isolation and molecular identification of R. mucilaginosus from salted cheese whey. The carotenoid pigments of yeasts accumulate in lipid droplets and can thus be extracted with various organic solvents. In general, efficient extraction of carotenoids from microbial cells still proves difficult as there is no standard technique. The extraction of the intracellularly produced carotenoids of yeast generally requires efficient disruption of the rigid cell wall of the yeast. Acid treatment may be used to disrupt the cellular membranes of yeast cells. Unfortunately, acid

treatment may result in considerable carotenoid damage. Other carotenoid extraction methods have also been reported based on enzymatic cell wall disruption [34,35] and supercritical carbon dioxide extraction [36]. It is plausible that some solvents, together to disrupt cells, when used demonstrate synergistic interactions, resulting in enhanced carotenoid yield. Sharma and Ghoshal reported that the maximum amount of carotenoids obtained in aerobic fermentation conditions was 819.23 mg/g compared 717.35 mg/g in a shake flask under similar conditions. The pigmented yeast samples were isolated from different sources such as flowers, tree exudates, fruits, and cheese [38]. One of which was identified as Rhodotorula agglutinins. Similar studies by Maldonade et al. [39] isolated pigmented yeasts from

Table 4 Histopathology scoring of Ehrlich solid tumor in response to treated with natural pigment alone or with radiation exposure

	•			
Group	Necrosis (%)	Neovascularization	Leukocytes	Fibrosis
Group 1: control	_	_	_	_
Group 2: MBST	10–15	++	+	_
Group 3: MBST+GMMP	35–50	+	++	++
Group 4: MBST+Radiation	25–30	_	+	_
Group 5: MBST+Radiation+GMMP	45–75	_	+	+++

soil, leaves, fruit, flowers, and processed food. Based on the spectral analysis ( $\lambda_{max}$ ) and the literature available, it can be concluded that the pigment of the yeast might be  $\beta$ -carotene and this result was in agreement with the finding of Parmar et al. [40], who reported that the UV-Vis spectrum of pigment of actinomycete was found by UV-Vis spectrophotometer. The spectra showed  $l_{max}$  at 277.44.

The terpenoidal oxygenated carotenoids may produce similar fragments with some other diagnostic ones for hydrocarbon unsaturted cyclic or open chain carotenes. It is worth mentioning that definite product fragments may be sufficient with other output parameters for accurate structural elucidation, even stereostructural features [41,42] after their matching with a respectable library database [43]. Like all microbial genera, Rhodotrula was reported to biosynthesize isoprenoids (isoprenoid quinones, carotenoids) as chemotaxonomic biomarkers for characterization and distinguishing their species [43]. This was in good agreement with the metabolites identified herein from R. mucilaginosa GMM, that is, 11 carotenoids (22, 23, 26, 28, 30, 33, 35–39), six long-chain fatty acids (7, 21, 31, 32, 34, 40), and a long-chain alkyl pbenzoguinones (25). The carotenoids identified as astraxanthin (22),4,4'-E-diapophytoene torularhodin (26), 1,2,1',2'-tetrahyroxylycopene (28), E-β-apo-8'-Ccrotenal (30), 10'-apo-E-β-caroten-10'ol (33), β-carotene (35), torulene (36), echinenone (37), 1,2,1',2'-tetrahyroxydihydrolycopene (38), and  $\alpha$ -canthaxanthin (39).

Carotenoids can be classified as carotenes and xanthophylls, the former (carotene, torulene, and lycopene) being pure hydrocarbons while the latter (lutein, zeaxanthin, violaxanthin, and neoxanthin) are oxygenated hydrocarbon derivatives [44,45]. β-carotene is an isoprenoid molecule with a chemical formula of C<sub>40</sub>H<sub>56</sub> with a molecular weight of 536.88 g/mol. This chemical is composed of two β-ionone rings linked together by a polyene chain with nine conjugated double bonds. The chemical β-carotene exhibits a peak absorbance at 450 nm and is distinguished by its hue, ranging from yellow to orange, owing to its molecular structure arrangement of double bonds [46] mucilaginosa [47] are also known for efficiently producing microbial β-carotene. Astaxanthin is classified as a xanthophyll with a molecular formula of  $C_{40}H_{52}O_4$  and a molar mass of 596.85 g/mol.

The structure consists of two polar  $\beta$ -ionone rings linked by a nonpolar chain. Each ring consists of a single hydroxyl group and a single ketone group. The astaxanthin molecule contains a total of 13 double bonds, which contribute to its potent antioxidant effects. Astaxanthin possesses ketone and hydroxyl groups, which enable it to undergo esterification and dictate its polar nature. Astaxanthin is an optically active molecule because it contains hydroxyl groups in the β-ionone rings. Astaxanthin exhibits three isomers due to the presence of chiral centers at positions C-3 and C-3': enantiomers (3 S, 3'S, and 3 R, 3'R) and a meso form (3 R, 3'S) (no. 33–35). The primary fungal producer of this chemical is the Xanthophyllomyces dendrorhous yeast, which predominantly synthesizes the (3 R, 3'R) isomer [48]. With a molecular formula of C40H54 and a molar mass of 534.9 g/mol, Torulene is classified as a member of the carotenes group. The torulene molecule comprises a single β-ionone ring connected to a polyene chain with 12 conjugated double bonds. The hue of the substance varies between orange and orange-red, depending on its concentration. The Rhodotorula genus's yeasts are torulene's primary microbiological producers [49]. Torulene exhibits antioxidant and anticancer characteristics [50]. The methanolic extract's DPPH radical scavenging capacity is compared with that of ascorbic acid. Ascorbic acid showed high activity with IC50 from a concentration of less than 20 µg/ml at 30 min. Using the DPPH assay, earlier reports showed comparable IC50 values for astaxanthin 79.32-18.10, lutein 35, and zeaxanthin 10 mg/ml [51]. Carotenoids function as antioxidants, actively seeking out and neutralizing free oxygen radicals within the body. Administration of carotenoid complex supplementation for 8 weeks effectively mitigated oxidative stress in a sample of trial participants of healthy individuals, athletes, and pregnant women [52]. This study aimed to investigate whether a carotenoid pigment from yeast could help fight cancer when mixed with low-dose radiation, focusing on ovarian cancer cells in particular. Our comprehensive analysis sheds light on the therapeutic implications potential of combination regimen. Our results showed that the combined treatment of carotenoid pigment and lowdose radiation effectively reduced the viability of ovarian cancer cells in a dose-dependent manner. The cell viability assay showed that the combination treatment significantly reduced cell viability compared with the control group. The antioxidant activity of GMMP from the ORAC assay yielded promising results. GMMP exhibited a substantial antioxidant capacity with an ORAC value of 1 610 991 µM TE/ mg sample. These findings align with several studies highlighting the antioxidant potential of natural

compounds. For example, it has been demonstrated that polyphenols, flavonoids, and carotenoids present in various plant-derived substances can exhibit antioxidant properties by preventing the formation of ROS and protecting against oxidative stress [53]. The ORAC assay has been widely used to evaluate the antioxidant capacity of natural compounds, making it a suitable method for assessing GMMP in this context. The in-vitro anticancer activity of GMMP, particularly against the CAOV-3 ovarian cancer cell line, revealed significant antiproliferative effects. This aligns with previous studies that have explored the anticancer potential of natural compounds. Khan et al. [54] emphasized the importance of herbal medicinal medications, noting their potential to prevent and treat cancer. The MTT assay results demonstrated that GMMP exhibited a robust inhibitory impact on CAOV-3 cells, with an  $IC_{50}$  value of 0.697 µmol/ml. These findings are consistent with those of Luithui et al. [55], who reported that natural compounds derived from herbs can minimize cancer cell viability. In the mouse model of solid Ehrlich tumors, GMMP, combined with radiation, significantly reduced tumor weight and volume. This corroborates the findings of Seyfried and Huysentruyt [56], who highlighted the importance of targeting tumor growth and metastasis as critical strategies in cancer therapy. The dual treatment approach exhibited the highest decrease ratio, emphasizing the potential synergistic effects of GMMP and radiation in inhibiting tumor progression.

The balance between BAX and anti-BCL2 proteins is crucial in determining cell fate. In our study, the CAOV-3 and radiation group exhibited the highest BAX expression, while the CAOV-3 without the treatment group had the highest BCL2 levels. These findings indicate that radiation promotes apoptosis in CAOV-3 cells, which is consistent with previous studies [57]. However, the combination of GMMP and radiation demonstrated a substantial increase in BAX expression, suggesting enhanced apoptotic potential. The results emphasize the combined effects of GMMP and radiation in stimulating apoptosis, a crucial method for suppressing the growth of cancer cells.

P53, a tumor suppressor gene, is pivotal in DNA repair, cell cycle regulation, and apoptosis induction [58] Our results revealed significant variations in P53 expression among treatment groups. The study investigated the impact of GMMP and radiation therapy on tumor characteristics, focusing on P53 expression, matrix metalloproteinases (MMPs), caspases, and histopathological changes in Ehrlich solid tumors. The results revealed significant variations in P53 expression among treatment groups, with the HEK-293 treated by GMMP and irradiated group showing the highest expression. This finding suggests a potential role of GMMP and radiation in activating P53-mediated pathways, which are known to contribute to suppression. MMPs, particularly MMP2 MMP9, are associated with tumor invasion and metastasis [59]. Regarding MMPs, MMP2 levels were significantly elevated in the CAOV-3 without the treatment group, indicating potential variations in MMP regulation. However, MMP9 levels did not significant differences between groups, suggesting that GMMP and radiation may not strongly influence its expression in these cells.

The study also found significant alterations in caspases, with the CAOV-3 treated by GMMP and irradiated group exhibiting the highest levels of caspase-3 and caspase-9. This indicates an enhanced apoptotic response to combined treatment, which aligns with the increased BAX expression and underscores the potential of GMMP and radiation in promoting apoptosis, a critical mechanism for inhibiting cancer cell survival. In terms of histopathological findings, untreated Ehrlich solid tumors exhibited characteristic features of malignancy, including dense clustering and infiltration of adjacent tissues. In contrast, treated tumors showed notable degenerative changes, including vacuolation of neoplastic cells, pyknosis, and karyolysis, indicative of apoptosis or necrosis. Inflammatory cell infiltration was also observed in treated tumors, suggesting a potential enhancement of the antitumor immune response [60].

# Conclusion

In this study, we produced the yeast natural pigment (GMMP) using fermentation and explored the potential therapeutic efficacy of GMMP in combination with radiation therapy against Ehrlich solid tumors. Our comprehensive investigations encompassed in-vitro and in-vivo experiments. This combination therapy exhibits multifaceted antitumor effects, including direct cytotoxicity, apoptosis induction, inhibition of metastatic potential, and immunomodulation. The results of our study underscore the potential of GMMP as a novel and promising adjunctive treatment strategy in the fight against solid tumors. Further investigations, including clinical trials, are warranted to fully elucidate the therapeutic mechanisms and optimize the application

of GMMP in cancer therapy. Thus, structural factors were significantly associated with antioxidant and anticancer efficacy.

# **Acknowledgments**

The authors extend their heartfelt appreciation to Prof. Dr Ahmed Othman, Professor of Pathology at the Faculty of Veterinary Medicine, University of Cairo, throughout invaluable support histopathological examination.

Authors' contributions: Ghada S. Ibrahim and Amal I. investigation, literature Hassan: searching, methodology, writing, and original draft. Manal G. Mahmoud: investigation, resources, conceptualization, methodology, writing, original draft, review, and editing. Mohsen M.S. Asker and Mohamed Marzouk: methodology, writing, and editing.

# Financial support and sponsorship Nil.

#### Conflicts of interest

There are no conflicts of interest.

#### References

- 1 Morin-Crini N, Lichtfouse E, Torri G, Crini G. Applications of chitosan in food, pharmaceuticals, medicine, cosmetics, agriculture, textiles, pulp and paper, biotechnology, and environmental chemistry. Environ Chem Lett
- 2 Black HS, Boehm F, Edge R, Truscott TG. The benefits and risks of certain dietary carotenoids that exhibit both anti- and pro-oxidative mechanisms-a comprehensive review. Antioxidants 2020: 9:264.
- 3 Shin J, Song MH, Oh JW, Keum YS, Saini RK. Pro-oxidant actions of carotenoids in triggering apoptosis of cancer cells: a review of emerging evidence. Antioxidants 2020; 9:532.
- 4 Kalra R, Gaur S, Goel M. Microalgae bioremediation: a perspective towards wastewater treatment along with industrial carotenoids production. J. Water Process Eng. 2021; 40:101794.
- 5 Konuray G., Erginkaya Z. Antimicrobial and antioxidant properties of pigments synthesized from microorganisms. In: Méndez-Vilas A, (eds) The battle against microbial pathogens: basic science,technological advances and educational programs. Spain: Formatex Research Center; 2015. pp. 27-30.
- 6 Maldonade IR, Rodriguez-Amaya DB, Scamparini AR. Statistical optimisation of cell growth and carotenoid production by Rhodotorula mucilaginosa. Braz J Microbiol 2012; 43:109-115.
- 7 Zhao Y, Guo L, Xia Y, Zhuang X, Chu W. Isolation, identification of carotenoid-producing Rhodotorula sp. from marine environment and optimization for carotenoid production. Mar Drugs 2019; 17:161.
- 8 Patel Y, Prakash AP, Patel AS, Vishwakarma SK. Pleurotus Species as source of nutraceuticals including vitamin B12 and lignocellulosic degradative enzyme. J. Biosci. Biotechnol. 2020; 9:33-46.
- 9 Dachtler M, Glaser T, Kohler K, Albert K. Combined HPLC-MS and HPLC-NMR on-line coupling for the separation and determination of lutein and zeaxanthin stereoisomers in spinach and in retina. Anal Chem 2001;
- 10 Pérez-López C, Rodríguez-Mozaz S, Serra-Compte A, Alvarez-Muñoz D, Ginebreda A, Barceló D, Tauler R. Effects of sulfamethoxazole exposure on mussels (Mytilus galloprovincialis) metabolome using retrospective nontarget high-resolution mass spectrometry and chemometric tools. Talanta 2023; 15:123804.
- 11 Salim RG, Fadel M, Youssef YA, Taie HAA, Abosereh NA, El-Sayed GM, Marzouk M. A local Talaromyces atroroseus TRP-NRC isolate: isolation,

- genetic improvement, and biotechnological approach combined with LC/ HRESI-MS characterization, skin safety, and wool fabric dyeing ability of the produced red pigment mixture. J Genet Eng Biotechnol 2022; 20:62.
- 12 El Sayed GH, Fadel M, Marzouk M. Optimization, a potential production, GC-MS and characterization of dark green pigment from new local isolate Streptomyces nigra strain GH12. J Adv Biol Biotechnol. 2023; 26:11-29.
- 13 Balakumar P. Maung-U K. Jagadeesh G. Prevalence and prevention of cardiovascular disease and diabetes mellitus. Pharmacol Res 2016; 113:600-609.
- 14 Elmehrath AO, Afifi AM, Al-Husseini MJ, Saad AM, Wilson N, Shohdy KS, et al. Causes of death among patients with metastatic prostate cancer in the US From 2000 to 2016. JAMA Netw Open 2021; 4:e2119568.
- 15 Yildizhan H, Barkan NP, Turan SK, Demiralp Ö, Demiralp FDÖ, Uslu B, Mzkan SA. Treatment strategies in cancer from past to present. In: Drug Target. Stimuli Sensitive Drug Deliv. Syst. Bucharest, Romania: Elsevier; 2018:1-37.
- 16 Olsen JE, Dineva SB. Effects of chronic ionizing radiation and interactions with other environmental and climatic factors on plant growth and development. eJ Appl Forest Ecol 2017; 5:31-53.
- 17 Obrador E, Salvador R, Villaescusa JI, Soriano JM, Estrela JM, Montoro A. Radioprotection and Radiomitigation: From the Bench to Clinical Practice. Biomedicines 2020; 8:461.
- 18 Hasanuzzaman M, Parvin K, Bardhan K, Nahar K, Anee TI, Masud AAC, Fotopoulos V. Biostimulants for the regulation of reactive oxygen species metabolism in plants under abiotic stress. Cells 2021; 10:2537.
- 19 Hayes JD, Dinkova-Kostova AT, Tew KD. Oxidative stress in cancer. Cancer cell 2020; 38:167-197.
- 20 Yamamoto N, Yamamoto N, Amemiya H, Yokomori Y, Shimizu K, Totsuka A. Electrophoretic karyotypes of wine yeasts. Am J Enol Vitic 1991;
- 21 Esteve-Zarzoso B, Belloch C, Uruburu F, Querol A. Identification of yeasts by RFLP analysis of the 5.8S rRNA gene and the two ribosomal internal transcribed spacers. Int J Syst Bacteriol 1999; 1:329-337.
- 22 Nunes AN, Do Carmo CS, Duarte CMM. Production of a natural red pigment derived from Opuntia spp. using a novel high pressure CO2 assisted-process. RSC Adv 2015; 5:83106-83114.
- 23 de Medeiros FO, Alves FG, Lisboa CR, de S, Martins D, Burkert CA, Kalil VSJ. Ultrasonic waves and glass pearls: a new method of extraction of beta-galactosodade for use in laboratory. Quim. Nova. 2008; 31:336-339.
- 24 Asker D. Ohta Y. Production of canthaxanthin by extremely halophilic bacteria. J Biosci Bioeng 1999; 88:617-21.
- 25 Mohammed HA, Khan RA, Abdel-Hafez AA, Abdel-Aziz M, Ahmed E, Enany S, et al. Phytochemical profiling, in vitro and in silico antimicrobial and anti-cancer activity evaluations and Staph GyraseB and h-TOP-IIB receptor-docking studies of major constituents of Zygophyllum coccineum L. Aqueous-ethanolic extract and its subsequent fractions: an approach to validate traditional phytomedicinal knowledge. Molecules 2021; 26:577
- 26 Brand-Williams W, Cuvelier ME, Berset C. Use of a free radical method to evaluate antioxidant activity. LWT-Food Sci Technol 1995;
- 27 Liang Z, Cheng L, Zhong GY, Liu RH. Antioxidant and antiproliferative activities of twenty-four Vitis vinifera grapes. PLoS One 2014; 9:e105146.
- Mosmann T. Rapid colorimetric assay for cellular growth and survival: application to proliferation and cytotoxicity assays. J Immunol Methods 1983; 65:55-63.
- 29 Mansour SZ, Anis LM. Possible effect of 5, 6-dimethyl-4 isothiocyanate thieno [2, 3-d] pyrimidine and I or irradiation on Ehrlich carcinoma in mice. J Radic Res Appl Sci 2010; 3:599-618.
- 30 Nabil HM, Hassan BN, Tohamy AA, Waaer HF, Abdel Moneim AE. Radioprotection of 1, 2-dimethylhydrazine-initiated colon cancer in rats using low-dose  $\gamma$  rays by modulating multidrug resistance-1, cytokeratin 20, and β-catenin expression. Human Exp Toxicol 2016; 35:282-
- 31 Goto T, Nishi T, Tamura T, Dev SB, Takeshima H, Kochi M, et al. Highly efficient electro-gene therapy of solid tumor by using an expression plasmid for the herpes simplex virus thymidine kinase gene. Proc Natl Acad Sci U S A 2000: 97:354-359.
- 32 Benzie IF, Strain JJ. The ferric reducing ability of plasma (FRAP) as a measure of 'antioxidant power': the FRAP assay. Anal Biochem 1996; 239:70-76
- 33 Kanzy HM, Nasr NF, El-Shazly HAM, Barakat OS. Optimization of carotenoids production by yeast strains of Rhodotorula using salted cheese whey. Int J Curr Microbiol App Sci 2015; 4:456-469.

- 34 Yurkov AM, Vustin MM, Tyaglov B, Maksimova VIA, Sineokiy SP. Pigmented basidiomycetous yeasts are a promising source of carotenoids and ubiquinone Q 10. Microbiology 2008; 77:1-6.
- 35 Ungureanu C, Marchal L, Chirvase AA, Foucault A. Centrifugal partition extraction, a new method for direct metabolites recovery from culture broth: case study of torularhodin recovery from Rhodotorula rubra. Bioresour Technol 2013: 132:406-409.
- 36 Simova ED, Frengova GI, Beshkova DM. Synthesis of carotenoids by Rhodotorula rubra GED8 co-cultured with yogurt starter cultures in whey ultrafiltrate. J Ind Microbiol Biotechnol 2004; 31:115-121.
- Sharma R, Ghoshal G. Optimization of carotenoids production by Rhodotorula mucilaginosa (MTCC-1403) using agro-industrial waste in bioreactor: a statistical approach. Biotechnol Rep 2019; 25:e00407.
- 38 El-Banna AA, Abd El-Razek AM, El-Mahdy AR, Isolation, identification and screening of carotenoid-producing strains of Rhodotorula glutinis. Food Nutr Sci 2012; 3:627-633.
- 39 Maldonade IR, Scamparini ARP, Rodriguez-Amaya DB. Selection and characterization of carotenoid-producing yeasts from Campinas region, Brazil. Braz J Microbiol. 2007; 38:65-70.
- 40 Parmar P. Singh AK, Meena GS, Borad S, Raiu PN, Application of ohmic heating for concentration of milk. J Food Sci Technol 2018; 55:4956-4963.
- Ramesh R, Kathiravan C, Chellasamy EE. Circular polarization observations of type II solar radio bursts and the coronal magnetic field. Astrophysical J 2022; 932:48.
- 42 Bach E, Schymanski EL, Rousu J. Joint structural annotation of small molecules using liquid chromatography retention order and tandem mass spectrometry data. Nat. Mach. Intell 2022; 4:1224-1237.
- 43 Ramesh C, Prasastha VR, Venkatachalam M, Dufossé L. Natural substrates and culture conditions to produce pigments from potential microbes in submerged fermentation. Fermentation 2022: 8:460.
- Olatunde A, Tijjani H, Ishola AA, Egbuna C, Hassan S, Akram M. Carotenoids as functional bioactive compounds. Funct Nutraceuticals Bioact Components Formul. Innov 2020:415-444.
- Singh A, Mukherjee T. Application of carotenoids in sustainable energy and green electronics. Mater Adv 2022; 3:1341-1358.
- Chel-Guerrero L, Estrella-Millán Y, Betancur-Ancona D, Aranda-González I, Castellanos-Ruelas A, Gallegos-Tintoré S. Antioxidant, chelating, and angiotensin-converting enzyme inhibitory activities of peptide fractions from red lionfish (Pterois volitans L.) muscle protein hydrolysates. Int Food Res J 2020; 27:224-233.
- 47 Gupta I, Adin SN, Panda BP, Mujeeb M.  $\beta$ -Carotene-production methods, biosynthesis from Phaffia rhodozyma, factors affecting its production during

- fermentation, pharmacological properties: a review. Biotechnol Appl Biochem 2022; 69:2517-2529
- 48 Rodríguez-Sáiz M, de la Fuente JL, Barredo JL. Xanthophyllomyces dendrorhous for the industrial production of astaxanthin. Appl Microbiol Biotechnol 2010; 88:645-658.
- 49 Barredo JL, García-Estrada C, Kosalkova K, Barreiro C. Biosynthesis of astaxanthin as a main carotenoid in the heterobasidiomycetous Yeast Xanthophyllomyces dendrorhous. J Fungi 2017; 3:44.
- 50 Du C, Guo Y, Cheng Y, Han M, Zhang W, Qian H. Torulene and torularhodin, protects human prostate stromal cells from hydrogen peroxide-induced oxidative stress damage through the regulation of Bcl-2/Bax mediated apoptosis. Free Radic Res 2017; 51:113-123.
- 51 Neumann U, Derwenskus F, Flaiz Flister V, Schmid-Staiger U, Hirth T, Bischoff SC. Fucoxanthin, a carotenoid derived from Phaeodactvlum tricornutum exerts antiproliferative and antioxidant activities in vitro. Antioxidants 2019; 8:183.
- 52 Zhuang C, Yuan J, Du Y, Zeng J, Sun Y, Wu Y, et al. Effects of oral carotenoids on oxidative stress: a systematic review and meta-analysis of studies in the recent 20 years. Front Nutr 2022; 9:754707.
- 53 Michalak M. Plant-derived antioxidants: significance in skin health and the ageing process. Int J Mol Sci 2022; 23:585.
- 54 Khan S, Sharaf M, Ahmed I, Khan TU, Shabana S, Arif M, et al. Potential utility of nano-based treatment approaches to address the risk of Helicobacter pylori. Expert Rev Anti Infect Ther 2022; 20:407-424.
- 55 Luithui Y, Kamani MH, Sreerama YN, Meera MS. Impact of hydrothermal processing on squalene.  $\alpha$ -tocopherol, and fatty acid content in Job's tears grain milled fractions: evaluation of their storage stability. J Sci Food Agric 2021; 101:2319-2327.
- 56 Seyfried TN, Huysentruyt LC. On the origin of cancer metastasis. Crit Rev Oncog 2013: 18:43-73
- Morrison BH, Bauer JA, Hu J, Grane RW, Ozdemir AM, Chawla-Sarkar M, et al. Inositol hexakisphosphate kinase 2 sensitizes ovarian carcinoma cells to multiple cancer therapeutics. Oncogene 2002; 21:1882-1889
- Yogosawa S, Yoshida K. Tumor suppressive role for kinases phosphorylating p53 in DNA damage-induced apoptosis. Cancer Sci 2018; 109:3376-3382.
- 59 Brown GT, Murray GI. Current mechanistic insights into the roles of matrix metalloproteinases in tumour invasion and metastasis. J Pathol 2015: 237:273-281.
- 60 Sheikh Z. Brooks PJ. Barzilav O. Fine N. Glogauer M., Macrophages. foreign body giant cells and their response to implantable biomaterials. Materials 2015; 8:5671-5701.